

# Photocatalytic Degradation of Methylene Blue Using ZnO-Based Composites: Evaluating the Efficiency of ZnO, ZnO-TiO<sub>2</sub>, and ZnO-TiO<sub>2</sub>-aCFA/Biochar

Fezile Nkosi\*, and Yusuf Isa

University of the Witwatersrand, Johannesburg, South Africa

## \*Corresponding author:

Fezile Nkosi, University of the Witwatersrand, Johannesburg, South Africa.

## ABSTRACT

This study evaluates the photocatalytic performance of ZnO, ZnO-TiO<sub>2</sub>, and ZnO-TiO<sub>2</sub>-Biochar composites for methylene blue degradation under simulated solar light. Characterization techniques (SEM, XRD, and FTIR UV-Vis) confirmed structural and surface properties, while photocatalytic tests assessed efficiency, kinetics, and reusability. ZnO-TiO<sub>2</sub>-Biochar showed the highest degradation, achieving 100% removal in 15 minutes, outperforming ZnO-TiO<sub>2</sub> (25 min) and ZnO (45 min), due to enhanced light absorption, improved charge separation, and higher adsorption capacity. Optimal conditions included room temperature, neutral pH, moderate catalyst loading (0.35 g/L), and low dye concentration. Reactive species studies identified hydroxyl radicals, superoxide anions, and photogenerated holes as the primary active species. The composite also demonstrated good structural stability and reusability, highlighting its potential as a cost-effective and eco-friendly photocatalyst for wastewater treatment.

**Keywords:** Electromagnetic Cloaking, AI-Based Inverse Design, Deep Neural Networks (DNN), Transformation Optics, Radar Cross Section (RCS) Reduction, Intelligent Metamaterial Engineering.

Received: May 06, 2026;

Accepted: May 12, 2026;

Published: May 19, 2026

## Introduction

### Background

The release of synthetic dyes like methylene blue (MB) in wastewater from textile and industrial processes, significantly threatens environmental and human health due to their toxicity, persistence, and resistance to conventional treatment methods. MB, a common cationic dye, is typically used as a pollutant to assess the efficiency of photocatalytic materials [1]. Photocatalysis has shown great promise as a sustainable and effective approach for the degradation of these dyes, with zinc oxide (ZnO) gaining attention for its photocatalytic activity under ultraviolet and solar irradiation. However, ZnO faces limitations such as fast recombination electron-hole pairs, and this reduces its photocatalytic efficiency [2]. To overcome

these limitations, composite materials such as ZnO combined with titanium dioxide (TiO<sub>2</sub>) have been extensively studied. TiO<sub>2</sub> has been widely studied as a photocatalyst for the degradation of organic contaminants and the generation of renewable fuels from water and carbon dioxide [3,4]. TiO<sub>2</sub> not only enhances charge separation but also broadens the light absorption range, resulting in improved photocatalytic performance [5]. In addition, the incorporation of biochar as support materials provides increased adsorption capacity and catalyst stability, facilitating greater contact between pollutants and active sites [6,7]. The removal of dyes from wastewater is critically important due to the environmental and health hazards caused by dye pollutants discharged from industries such as textile, leather tanning, and cosmetics.

**Citation:** Fezile Nkosi, and Yusuf Isa (2026) Photocatalytic Degradation of Methylene Blue Using ZnO-Based Composites: Evaluating the Efficiency of ZnO, ZnO-TiO<sub>2</sub>, and ZnO-TiO<sub>2</sub>-aCFA/Biochar. *J Mat Sci Ener Adva* 1: 1-5.

---

## Materials and Methods

### Materials

Zinc nitrate hexahydrate ( $\text{Zn}(\text{NO}_3)_2 \cdot 6\text{H}_2\text{O}$ ),  $\text{TiO}_2$ , NaOH, acetic acid ( $\text{CH}_3\text{COOH}$ ), and MB dye were purchased from a Chemicals shop (Sigma Aldrich). Biochar was synthesized from sawdust to act as a support material. Distilled water was used for all solution preparations and washing processes. All chemicals were laboratory grade. Glassware, magnetic stirrers, centrifuge tubes, syringe filters (0.45  $\mu\text{m}$ ), and cuvettes were used throughout.

### Materials Preparation & Synthesis

#### ZnO Nanoparticles (co-precipitation)

ZnO was synthesized through precipitation.  $\text{Zn}(\text{NO}_3)_2 \cdot 6\text{H}_2\text{O}$  was introduced in distilled water. Separately, sodium hydroxide (NaOH) solution was prepared in distilled water to form a second solution. Under vigorous stirring the first solution was added drop by drop to the second solution until pH of 10 was achieved. The suspension was stirred further for at least an hour to reach complete precipitation. The resulting white precipitate was separated using filter papers, washed at least five times with both distilled waters to remove impurities, and then later dried at approximately 70 °C overnight in an oven. The sample was then calcined in air at 400 °C for 3 hours at a heating rate of 5 °C  $\text{min}^{-1}$  to ensure crystalline ZnO nanoparticles.

#### ZnO-TiO<sub>2</sub> Composite

ZnO-TiO<sub>2</sub> composites were synthesized via the precipitation approach. The ZnO powder synthesized earlier was dispersed in distilled water under magnetic stirring. This was followed by the adding TiO<sub>2</sub> powder to obtain the desired ZnO: TiO<sub>2</sub> ratio (1:1 by weight). The mixture was stirred for 30 minutes until homogeneous dispersion was achieved. Centrifugation and drying at 80 °C overnight (24 hours) followed. ZnO-TiO<sub>2</sub> composites are often calcined at moderate temperatures (400–500 °C) to enhance crystallinity and photocatalytic properties [8]. Hence, the obtained solid was calcined at 450 °C for a maximum of 4 hours so an interparticle bonding is enhanced and crystallinity is achieved.

#### Biochar

Sawdust was air dried for 24 hours and then later milled. After grinding, sieving was done to ensure a particle class of 75  $\mu\text{m}$  to 200  $\mu\text{m}$ . The sawdust was later pyrolysed in a muffle furnace in an oxygen limited environment at 500 °C for 3 h (heating rate 5–10 °C  $\text{min}^{-1}$ ). Drying and mild calcination was done to stabilize composite structure without damaging the biochar support [6]. The resulting product (biochar) was ground into fine powder and stored in an airtight container prior to use.

#### Loading ZnO-TiO<sub>2</sub> onto Biochar (Impregnation)

Biochar was dispersed properly. ZnO-TiO<sub>2</sub> precursor solution was loaded through the method of incipient wetness impregnation. The ratio of catalyst to biochar was ensured to be 4:1. The mixture was stirred for 2 hours, gently heated (due to ethanol presence), dried at 70 °C and calcined at 400 °C for 3 h to improve adhesion while limiting support carbon burn-off. This resulted in ZnO-TiO<sub>2</sub>-Biochar. Combining biochar and ZnO-TiO<sub>2</sub> enhances pollutant adsorption and provides more active sites, strengthening the synergistic effect for improved photocatalytic degradation [9].

### Catalyst Characterisation

Scanning Electron Microscopy is widely employed to examine surface morphology and particle size, revealing features such as nanoflake-like ZnO, mesoporous TiO<sub>2</sub> clusters, and well-dispersed nanoparticles on biochar supports. The structure, morphology, and optical properties of the synthesized catalysts were analysed using X-ray diffraction (XRD), SEM, FTIR and UV-Vis spectroscopy. XRD was used to determine crystallinity and phase composition, SEM for surface morphology, and UV-Vis for optical absorption behavior and band gap estimation.

### Photocatalytic Experiments

Photocatalytic activity was evaluated under simulated solar irradiation using a 200 W xenon lamp. Typically, the reaction mixture consisted of 100 mL of methylene blue (MB, 10 mg  $\text{L}^{-1}$ ) and catalyst (0.35 g  $\text{L}^{-1}$ ), which was stirred continuously under irradiation [10-12]. Aliquots (3 mL) were withdrawn at 5-minute intervals, centrifuged to remove catalyst particles, and analysed spectrophotometrically at 664 nm. Control experiments were performed under three conditions: (i) MB solution under light with no catalyst, (ii) MB solution with catalyst in the dark, and (iii) MB solution with catalyst under irradiation. To determine the most efficient photocatalyst, all three synthesized materials (ZnO, ZnO-TiO<sub>2</sub>, and ZnO-TiO<sub>2</sub>-Biochar) were evaluated under identical experimental conditions. Each experiment was conducted using a 10ppm methylene blue (MB) solution, a catalyst mass of 35 mg, and a neutral pH at room temperature under simulated solar irradiation.

### Reusability of ZnO-TiO<sub>2</sub>-Biochar

In this study, the ZnO-TiO<sub>2</sub>-Biochar composite was subjected to three successive photocatalytic degradation cycles using methylene blue (MB) under simulated solar irradiation. After each cycle, the catalyst was then separated using a centrifuge, thoroughly washed with ethanol and distilled water to remove residual dye molecules, and then dried prior to reuse. The reusability of ZnO-TiO<sub>2</sub>-Biochar was evaluated through repeated photocatalytic degradation experiments of methylene blue under simulated solar irradiation. After each photocatalytic cycle, the photocatalyst was separated by centrifugation at 4000 rpm for 15 min, washed thoroughly with distilled water and ethanol to remove residual dye molecules, and dried at 70 °C for 2 h. The recovered photocatalyst was then reused under identical experimental conditions for up to three consecutive cycles.

## Results and Discussion

### Catalyst Characterization

#### XRD

The XRD analysis confirmed the successful synthesis and crystalline structure of ZnO, TiO<sub>2</sub>, and ZnO-TiO<sub>2</sub>-Biochar composites. ZnO exhibited sharp peaks at 31.8°, 34.4°, and 36.3° (2 $\theta$ ), corresponding to the (100), (002), and (101) planes of the hexagonal wurtzite phase (JCPDS 36-1451), indicating high crystallinity and phase purity with an average crystallite size of 33.1 nm. TiO<sub>2</sub> displayed typical anatase phase peaks at 25.3°, 37.8°, 47.8°, and 54.8° (2 $\theta$ ), consistent with JCPDS 21-1272. The ZnO-TiO<sub>2</sub>-Biochar composite showed combined reflections of ZnO and TiO<sub>2</sub>, confirming heterojunction formation, along with a broad peak at 24–26° attributed to amorphous carbon

from biochar, indicating successful incorporation of the carbon matrix, which enhances surface area and light absorption.

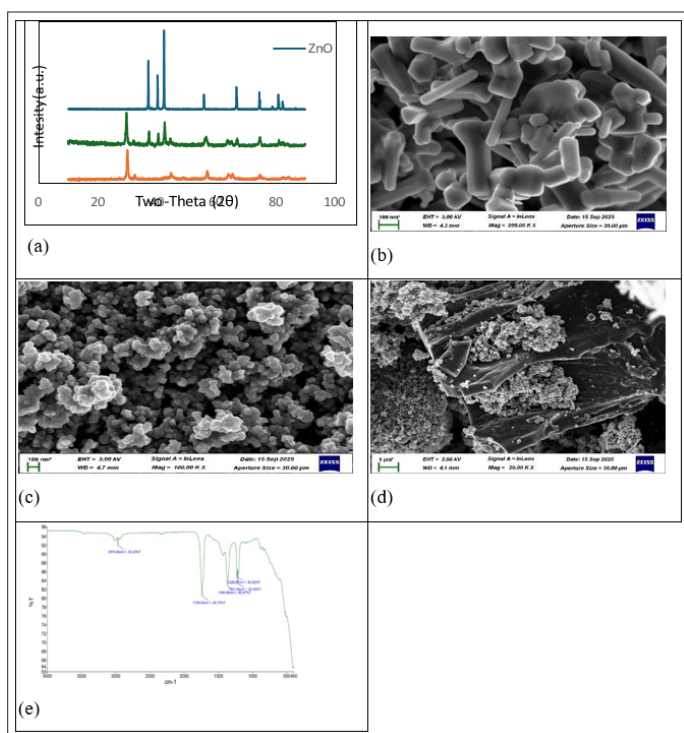


**Figure 1:** (a) XRD pattern of ZnO, ZnO-TiO<sub>2</sub> and ZnO-TiO<sub>2</sub>-Biochar. (b) SEM image of TiO<sub>2</sub>. (c) SEM image of ZnO. (d) SEM image of ZnO-TiO<sub>2</sub>-Biochar. (e) FTIR of ZnO-TiO<sub>2</sub>-Biochar

### SEM (Scanning Electron Microscopy)

The surface morphology of the ZnO-TiO<sub>2</sub>-Biochar composite observed through SEM on figure 1(d) reveals a heterogeneous structure, where ZnO and TiO<sub>2</sub> nanoparticles were uniformly dispersed across the porous biochar surface. The biochar provided a matrix that facilitated strong anchoring and distribution of the semiconductor particles. This is to prevent agglomeration and enhance the available surface area for photocatalytic reactions.

### FTIR

The FTIR spectrum of the ZnO-TiO<sub>2</sub>-Biochar composite (Figure 1e) displays several characteristic absorption peaks, indicating the successful incorporation of metal oxides into the carbon-based matrix [13]. The broad absorption band between 3420 and 3450 cm<sup>-1</sup> is associated with O-H stretching vibrations, suggesting the presence of surface hydroxyl groups or adsorbed water molecules on both the biochar and metal oxide surfaces. The peak observed around 1630–1650 cm<sup>-1</sup> corresponds to C=O stretching vibrations of carbonyl or carboxyl groups, confirming oxygen-containing functional groups derived from the biochar. Additionally, the bands appearing near 1100–1000 cm<sup>-1</sup> are attributed to C-O stretching vibrations, representing the organic structure of the biochar [14].

### Adsorption Results

Dark adsorption experiments were initially conducted to assess the equilibrium adsorption of methylene blue onto the catalysts' surfaces before light irradiation. Notably, ZnO,

ZnO-TiO and ZnO-TiO<sub>2</sub>-Biochar showed very high adsorption capacity of 16.7%, 60% and 55% under dark conditions, this effectively masked the photocatalytic degradation contributions. As a result, full dark experiments were not performed for all parameter variations. Instead, representative dark adsorption tests were conducted separately for each catalyst to determine their adsorption-desorption equilibrium behaviour. To evaluate if the 10ppm MB would fully degrade in the dark alone with ZnO-TiO<sub>2</sub>, the dark experiment was done separately for 2 hours. There was no complete degradation after 2 hours and 87% degradation was obtained. This is one of the factors that warranted the introduction of light to assess if the light enhances the photocatalysis [15,16].

### Photocatalytic Activity

#### Comparison of Photocatalysts (ZnO vs ZnO-TiO<sub>2</sub> vs ZnO-TiO<sub>2</sub>-Biochar)

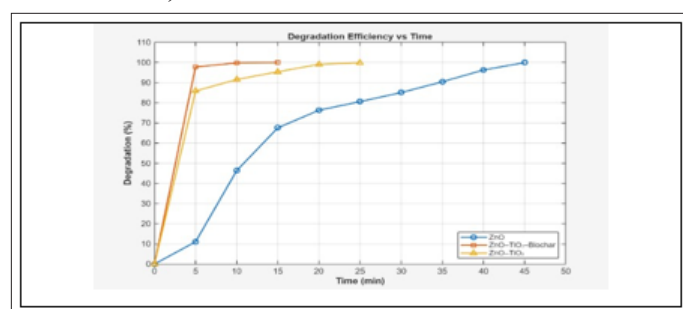


**Figure 2:** Degradation plot showing the efficiencies of the composites

The photocatalytic activity of the three catalysts was assessed under the same conditions (10 ppm methylene blue, 35 mg catalyst, neutral pH, room temperature) to determine the most efficient system. Figure 2 shows that ZnO-TiO<sub>2</sub>-Biochar achieved nearly complete degradation of methylene blue within 15 minutes, outperforming both ZnO-TiO<sub>2</sub> and ZnO. The bare ZnO exhibited the slowest degradation rate, reaching about 100% degradation after 45 minutes, whereas ZnO-TiO<sub>2</sub>-Biochar rapidly achieved 100% degradation after 25 minutes. The superior performance of ZnO-TiO<sub>2</sub>-Biochar can be attributed to synergistic effects such as enhanced charge separation, improved light utilization, greater adsorption capacity and an efficient transport of electrons.

### Effect of pH

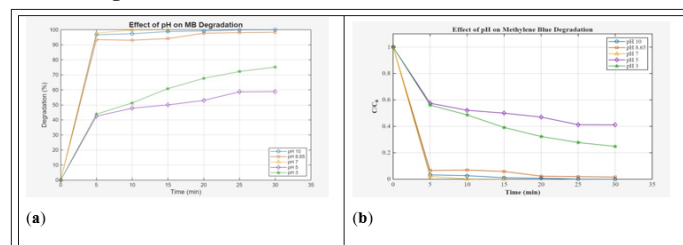


**Figure 3:** Degradation plots showing effect of pH

MB is a cationic dye that has an ionization state is positively charged across typical pH levels. Changes in pH can still affect the dye's adsorption behaviour and interaction with catalyst surface [17]. In acidic conditions, both the catalyst surface and MB

dye are positively charged, resulting in electrostatic repulsion, which reduces adsorption and degradation efficiency [18]. This is proven by the results in the graph above; in acidic levels 3 and, degradation efficiency is significantly lower compared to basic levels. And in neutral to alkaline conditions, electrostatic attraction dominates, facilitating better adsorption on the catalyst surface. This is evident from the results of neutral pH, which is optimum pH. This is highly advantageous for largescale applications.

### Effect of Temperature

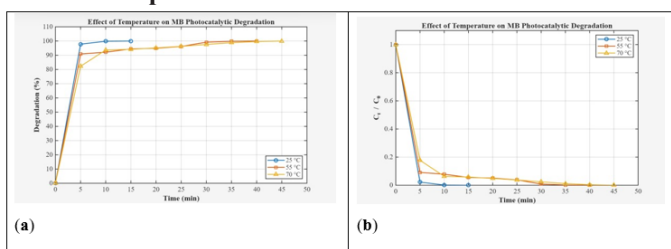


**Figure 4:** Degradation plot showing the effect of temperature

At 25 °C, the reaction reached complete degradation within 15 minutes, while at elevated temperatures (55 °C and 70 °C), the reaction proceeded further, achieving nearly 100% removal in 40 minutes and 45 minutes respectively.

### Effect of Initial Dye Concentration

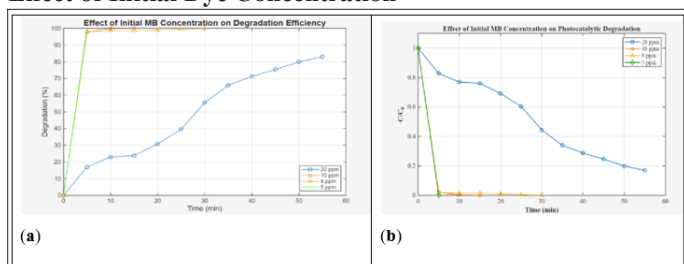


**Figure 5:** Degradation plot showing the effect of initial MB concentration

The effect of initial MB concentration on the degradation can be explained by light penetration and catalyst site saturation. At low concentrations (5 ppm), the solution is transparent, allowing effective light penetration and rapid catalyst activation, resulting in complete degradation within 5 minutes. At higher concentrations (10–20 ppm), increased light absorption reduces photon availability, and active sites on the catalyst become saturated with dye molecules. This limits adsorption and slows degradation, causing a plateau in both degradation efficiency and normalized concentration ( $C/C_0$ ) over time [19,20].

### Effect of Catalyst Dosage

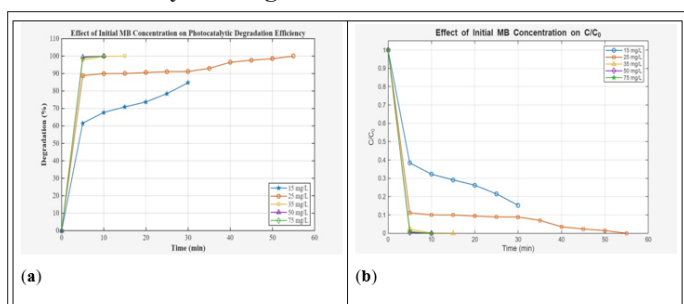


**Figure 6:** Degradation plot showing the effect of catalyst dosage

The effect of catalyst dosage on the degradation depends on active site availability and light scattering. Increasing catalyst dosage initially enhances degradation by providing more active sites for dye adsorption and reaction. However, beyond an optimal dosage, excess catalyst causes light scattering, shielding, and sometimes particle agglomeration, which reduce photon penetration and limit accessible active sites. Therefore, photocatalyst dosage must be optimized to balance sufficient active sites with minimal light attenuation, ensuring maximum degradation efficiency [12,21].

### Reusability of ZnO-TiO<sub>2</sub>-Biochar

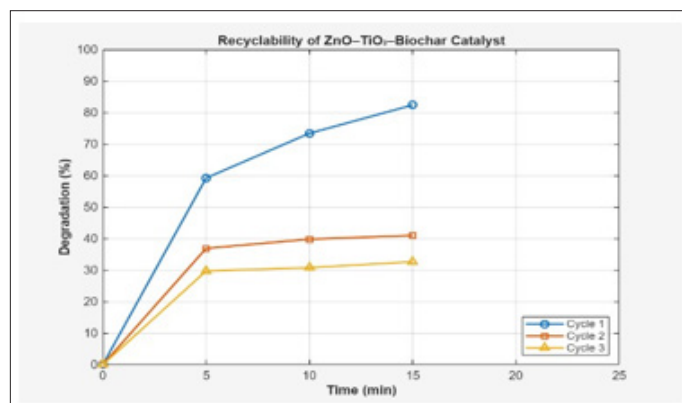


**Figure 7:** Reusability of ZnO-TiO<sub>2</sub>-Biochar

Multiple reuse cycles of ZnO-TiO<sub>2</sub>-Biochar composites show that structural stability and minimal performance loss are critical for wastewater treatment. Degradation efficiency decreased from 82% in the first cycle to 41% and 32% in the second and third cycles over 15 minutes, likely due to surface fouling and catalyst loss during recovery. Despite this decline, the composite retained significant activity, demonstrating good reusability. This makes it a robust, recyclable photocatalyst suitable for continuous or semi-continuous wastewater treatment, improving cost-effectiveness and reducing environmental impact.

### Reactive Species and Mechanism

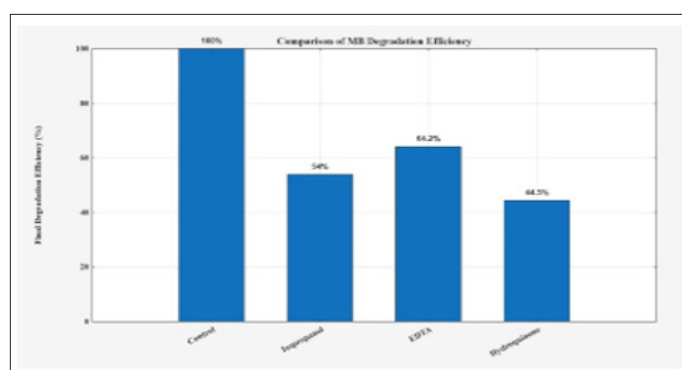


**Figure 8:** Chart showing the effect of the inhibitors on the degradation

Reactive oxygen species generated by these composites, especially hydroxyl radicals, drive organic dye breakdown consistent with accepted mechanisms [22]. Key reactive species generated include  $\cdot\text{OH}$ ,  $\text{O}_2^-$ , and  $\text{h}^+$ . Electrons reduce dissolved

oxygen to form  $O_2^-$ , while holes oxidize water or hydroxide ions to  $-OH$  [2]. Both radicals are highly oxidative and attack MB molecules, breaking them down into less toxic intermediates and ultimately mineralizing them to  $CO_2$  and  $H_2O$  [8].

## Conclusion

The ZnO–TiO<sub>2</sub>–Biochar composite demonstrates high photocatalytic efficiency for solar driven wastewater treatment, achieving rapid degradation because of the synergistic effects of TiO<sub>2</sub> heterojunctions (enhancing charge separation) and biochar (providing high surface area and adsorption sites). Scavenger studies identified hydroxyl radicals, photogenerated holes, and superoxide radicals as the main reactive species. The proved to be have excellent structural stability and has shown capabilities of reusability over multiple cycles. Kinetic analysis showed a pseudo-first-order degradation, with ZnO–TiO<sub>2</sub>–Biochar exhibiting the highest rate constant among the tested catalysts. These findings highlight its potential as a cost-effective, ecofriendly, and recyclable system for removing organic pollutants from water.

Future work could focus on extending this approach to other persistent dyes and real wastewater samples, as well as exploring scale-up potential for industrial wastewater remediation.

## References

1. Eswaran P, Madasamy P, Pillay K, Brink H (2024) 'Sunlight-driven photocatalytic degradation of methylene blue using ZnO/biochar nanocomposite derived from banana peels'. *Biomass Conversion and Biorefinery* 15: 12347–12367.
2. Krystynik P (2021) Advanced oxidation processes (AOPs) – utilisation of hydroxyl radical and singlet oxygen. *Biochemistry*. IntechOpen <http://dx.doi.org/10.5772/intechopen.98189>.
3. Al Jitan S, Palmisano G, Garlisi C (2020) Synthesis and surface modification of TiO<sub>2</sub>-based photocatalysts for the conversion of CO<sub>2</sub>. *Catalysts* 10: 227.
4. Jing L, Zhou W, Tian G, Fu H (2013) Surface tuning for oxide-based nanomaterials as efficient photocatalysts. *Chemical Society Reviews* 42: 9509–9549.
5. Dai J, Wu Y, Yao Y, Zhang B (2025) ZnO/TiO<sub>2</sub> photocatalysts for degradation of methyl orange by low-power irradiation. *Science progress* 108: 1-25.
6. Foong SY, Chin BLF, Lock SSM, Yiin CL, Tan YH, et al. (2024) Enhancing wastewater treatment with engineered biochar from microwave-assisted approach - A comprehensive review. *Environmental Technology & Innovation* 36: 103835.
7. Kumari K, Moyon NS, Ahmaruzzaman M (2025) Environmentally sustainable fabrication of SnO<sub>2</sub>/fly ash/biochar nanocomposite for enhanced photocatalytic performance for degradation of Ofloxacin and Rose Bengal. *Scientific reports* 15: 11965.
8. Khan I, Saeed K, Zekker I, Zhang B, Hendi AH, et al. (2022) Review on methylene blue: its properties, uses, toxicity and photodegradation. *Water* 14: 242.
9. Liu Y, Dai X, Li J, Shaoheng Cheng, Jian Zhang, et al. (2024) Recent progress in TiO<sub>2</sub>–biochar-based photocatalysts for water contaminants treatment: strategies to improve photocatalytic performance. *RSC Advances* 14: 3167–3189.
10. Lili Lu, Rui Shan, Yueyue Shi, Shuxiao Wang, Haoran Yuan (2019) A novel TiO<sub>2</sub>/biochar composite catalyst for photocatalytic degradation of methyl orange. *Chemosphere* 222: 391-398.
11. Mirabeau Shima, Kiani Maryam, Samavat Feridoun (2021) Structural Characterization and Synthesis of ZnO / TiO<sub>2</sub> Nano Composites. *International Journal of Thin Film Science and Technology* 10: 3-7.
12. Pereira MFR, Soares SF, Órfão JJM, Figueiredo JL (2003) Adsorption of dyes on activated carbons: influence of surface chemical groups. *Carbon* 41: 811–821.
13. Goncalves NP, Lourenco MA, Baleuri SR, Bianco S, Jagdale P, et al. (2022) Biochar waste-based ZnO materials as highly efficient photocatalysts for water treatment. *Journal of Environmental Chemical Engineering* 10: 107256.
14. Zhang S, Sun Z, Yao Y, Wang X, Tian S (2024) Spectral characterization of the impact of modifiers and different prepare temperatures on snow lotus medicinal residue-biochar and dissolved organic matter. *Scientific Reports* 14: 8493.
15. Vu TT, del Río L, Valdés-Solís T, Marbán G (2013) Stainless steel wire mesh supported ZnO for the catalytic photodegradation of methylene blue under ultraviolet irradiation. *Journal of Hazardous Materials* 246–247: 126–134.
16. Wongrerkrdee S, Boonruang C, Sujinnapram S (2022) Enhanced Photocatalytic Degradation of Methylene Blue Using Ti-Doped ZnO Nanoparticles Synthesized by Rapid Combustion. *Toxics* 11: 33.
17. Selvarajan E, Vairamuthu S (2021) Photocatalytic degradation of methylene blue using metal oxide catalysts: Role of pH and surface charge. *Journal of Environmental Chemical Engineering* 9: 104623.
18. Azeez F, Al-Hetlani E, Arafa M, Yasser Abdelmonem, Ahmed Abdel Nazeer, et al. (2018) The effect of surface charge on photocatalytic degradation of methylene blue dye using chargeable titania nanoparticles. *Sci Rep* 8: 7104.
19. Salehi M, Hashemipour H, Mirzaee M (2012) Experimental study of influencing factors and kinetics in catalytic removal of methylene blue with TiO<sub>2</sub> nanopowder. *American journal of environmental engineering* 2: 1-7.
20. Reza KM, Kurny A, Gulshan F (2017) Parameters affecting the photocatalytic degradation of dyes using TiO<sub>2</sub>: a review. *Applied Water Science* 7:1569–1578.
21. Khan S, Kiani H, Ahmad N, (2024) Photocatalytic Dye Degradation from Textile Wastewater. *ACS Omega* 9: 16573–16589.
22. Zhang Q, Liu Z, Chen Y, Wang L (2022) Nitrogen-Doped TiO<sub>2</sub>/Nitrogen-Containing Biochar Composite for Efficient Photocatalytic Degradation of Organic Pollutants. *ACS Omega* 7: 1200-1210.